

A novel triage-based fault diagnosis method for chemical process

Qucheng Tao^a, Bingru Xin^a, Yifan Zhang^a, Heping Jin^b, Qian Li^b, Zhongde Dai^c, Yiyang Dai^{a,*}

^a School of Chemical Engineering, Sichuan University, Chengdu 610065, China

^b China Three Gorges Corporation, Beijing 100038, China

^c School of Carbon Neutrality Future Technology, Sichuan University, Chengdu 610041, China



ARTICLE INFO

Keywords:

Fault diagnosis

Triage-based convolutional neural network

Tennessee Eastman process

Process safety

ABSTRACT

Deep learning-based fault detection and diagnosis (FDD) methods have received considerable attention, and many methods based on convolutional neural network (CNN) have been applied to fault diagnosis for chemical processes. However, current fault diagnosis methods train and detect all faults using a single model and the same feature inputs, resulting in the neglect of correlations and difference between faults and inferior fault diagnosis performance. In this study, a novel fault diagnosis method named triage-based convolutional neural network (TrCNN) for fault diagnosis is proposed. Initially, the fault set is partitioned into distinct triage types. Subsequently, distinct models are formulated and applied to their respective triage types in the sub networks layer, while a triage network is developed in the triage layer. Ultimately, the models from the triage layer and sub networks layer come together to constitute the triage fault diagnosis system. The proposed method can adaptively select suitable models and features for different triage types, leading to improved diagnostic accuracy, especially for similar faults. When applied to the Tennessee Eastman (TE) chemical process the TrCNN demonstrates impressive performance, validating its effectiveness in fault diagnosis.

1. Introduction

Process safety and risk management have always been major challenges faced by the process and manufacturing industries. To address this issue, digital systems have been applied to assist the process safety management throughout the entire lifecycle of process plants (Lee et al., 2019). The Fourth Industrial Revolution (Industry 4.0) is driving the automation, digitalization, and intelligence reform of process operations, control, and monitoring in the manufacturing industry (Espuña, 2018; Sansana et al., 2021). Although distributed control systems (DCS) and advanced process control (APC) can effectively monitor and control chemical processes, the management of abnormal operating conditions still relies heavily on manual operations, and approximately 70% of production accidents are caused by human errors (Quiñones-Grueiro

et al., 2019). Therefore, an intelligent abnormal operating conditions management system holds significant importance for the safety management of chemical processes.

Abnormal operating conditions refer to situations where the process deviates from the acceptable operating range. Because of the multivariable, strongly coupled, and nonlinear nature of chemical systems, the timely diagnosis and control of severe abnormal events present significant challenges (Hu et al., 2015). Arunthavanathan et al. proposed the application of fault detection and diagnosis (FDD) for managing abnormal operating conditions, which has become an indispensable method for ensuring safe and efficient production in chemical processes and holds significant theoretical and practical value in the chemical industry (Arunthavanathan et al., 2021; Bai and Zhao, 2023). Therefore, it is crucial to establish an intelligent,

Abbreviations: AE, Autoencoders; AIS, Artificial immune system; APC, Advanced process control; BiLSTM, Bi-directional long short-term memory; BN, Bayesian networks; CNN, Convolutional neural network; DBN, Deep belief network; DCNN, Deep convolutional neural network; DCS, Distributed control systems; EDCNN, Enhanced deep convolutional neural network; FDA, Fisher discriminant analysis; FDD, Fault detection and diagnosis; FDR, Fault detection rate; FPR, False positive rate; GAN, Generative adversarial network; GRU, Gated recurrent unit; KNN, K-nearest neighbors; LAE, Ladder autoencoder; LSTM, Long short-term memory; PCA, Principal component analysis; PDNN, Process dynamics-guided deep neural network; PLS, Partial least squares; PSO, Particle swarm optimization; PTCN, Process Topology Convolutional Network; ReLU, Rectified linear unit; RF, Random forest; RNN, Recurrent neural network; SRMBN, Strong relevant mechanism Bayesian network; SVM, Support vector machines; TE, Tennessee Eastman; TFD, Triage fault diagnosis; TrCNN, Triage-based convolutional neural network; t-SNE, T-distributed stochastic neighbor embedding.

* Corresponding author.

E-mail address: daiyy@scu.edu.cn (Y. Dai).

efficient, and robust FDD method for process safety in the chemical industry.

FDD methods can be categorized into three categories: model-based methods, knowledge-based methods, and data-driven methods. Model-based and knowledge-based methods have drawbacks such as strong reliance on experts, poor generalization capabilities, and difficulties in modeling. In contrast, data-driven methods rely less on expert knowledge and primarily depend on a large amount of measurable data available in the plant, making them simple and effective. With the continuous improvement of computing power and artificial intelligence, data-driven methods attracted more attention from researchers and became a popular research topic (Gordon et al., 2020).

Data-driven methods include statistical learning methods and machine learning methods. Among statistical learning methods, principal component analysis (PCA) has been widely applied due to its low computational cost and high fault detection rate (Jiang et al., 2016; Wise et al., 1990; Zhao et al., 2022). Additionally, partial least squares (PLS) (Kumar et al., 2003), Fisher discriminant analysis (FDA) (Chiang et al., 2004) and others have also been applied (Feng et al., 2022; Wang et al., 2021; Xiao et al., 2021). Machine learning methods include support vector machines (SVM) (Mahadevan and Shah, 2009; Yin and Hou, 2016), k-nearest neighbors (KNN) (Wang et al., 2015), random forest (RF) (Liu and Ge, 2018), and artificial immune system (AIS) (Yao et al., 2022). Fault diagnosis models based on Bayesian networks (BN) are interpretable models built on the foundation of Bayesian theory, and research progress has been made in this area (Amin et al., 2021a; Bi et al., 2022; Liu et al., 2022b). In the pursuit of ensuring process safety and risk assessments, there have been several improved approaches in this area. For example, Kaib et al. improved the kernel PCA-based algorithm to enhance its adaptability to nonlinear industrial processes through fractal dimension (Kaib et al., 2023). Ji et al. proposed a multimode process monitoring method based on DISS-PVC for the production loads in industrial operations are frequently adjusted (Ji et al., 2022). Hybrid methods, which combine two or more techniques, have also been used for FDD (Amin et al., 2021b). Due to the advantages of different methods, hybrid methods can often overcome the limitations of an individual method and achieve better results. The diverse combinations of hybrid risk assessment methods are also worthy of in-depth exploration. For example, Li et al. proposed a new Copula-Bayesian based hybrid approach for risk modeling of the decommissioning operation of subsea pipelines (Li et al., 2022). Liu et al. proposed a strong relevant mechanism Bayesian network (SRMBN) for fault detection and diagnosis and applied to TE (Liu et al., 2022a). However, due to limited model capacity, their ability to extract features from high-dimensional data is constrained, leading to specific limitations.

Compared to traditional machine learning methods, deep learning is more effective in feature extraction. It overcomes some limitations of shallow learning by obtaining hierarchical representations of raw data through multiple layers of nonlinear transformations. Deep learning algorithms in fault diagnosis include deep belief network (DBN) (Zhang and Zhao, 2017), convolutional neural network (CNN) (Wu and Zhao, 2018), recurrent neural network (RNN) (Zhang et al., 2020), and transformer (Wei et al., 2022). Furthermore, there have been several improved approaches in this area. For example, Zhang et al. proposed an LSTM-LAE method which combining long short-term memory (LSTM) and ladder autoencoder (LAE) that effectively utilizes unlabeled data to enhance fault diagnosis performance (Zhang and Qiu, 2022b). Zheng and Zhao introduced an improved confidence-based self-training algorithm, which improves the application of self-supervised learning in semi-supervised fault diagnosis (Zheng and Zhao, 2022). Wu et al. presented a Process Topology Convolutional Network (PTCN) model for complex chemical process fault diagnosis, simplifying the model construction process and enhancing interpretability (Wu et al., 2023; Wu and Zhao, 2021). Moreover, Alauddin et al. presented a process dynamics-guided deep neural network (PDNN) model to enhance model generalization by rendering process dynamics and field expertise

(Alauddin et al., 2023). Kopbayev et al. integrated CNN with Bi-directional long short-term memory (BiLSTM) to capture spatial then temporal features sequentially and applied it for gas leakage detection (Kopbayev et al., 2022). Furthermore, Zhang et al. designed a GRU-EDCNN model that combines the gated recurrent unit (GRU) with the enhanced deep convolutional neural network (EDCNN) (Zhang et al., 2023). In addition, new models such as autoencoders (AE) and generative adversarial network (GAN) have also been applied to fault diagnosis tasks, offering alternative approaches to address the challenges in this field (Bi and Zhao, 2021; Li et al., 2021).

Among the algorithms in deep learning, CNNs have advantages in extracting local features from process data and are also easier to converge during training (Jiao et al., 2020). CNNs have been widely applied in fault diagnosis tasks. Wu and Zhao transformed historical data into 2D data matrices with corresponding labels to construct a deep convolutional neural network (DCNN) fault diagnosis model that simultaneously extracts spatial and temporal features (Wu and Zhao, 2018). Deng et al. considered the influence of variable order on feature extraction and optimized the feature sequence and arrangement order using a genetic algorithm (Deng et al., 2021). Song and Jiang took into account the impact of convolutional kernel size and used a multi-scale CNN approach after transforming the data into 2D images for fault diagnosis (Song and Jiang, 2022). However, chemical process datasets consist of multiple variables, including temperature, pressure, liquid level, etc. These variables form a complex topological structure that cannot be easily represented using 2D graphs. Moreover, 2D convolutional kernels may lead to a decrease in feature extraction effectiveness along the time dimension, causing important information to be overlooked (Yu et al., 2020). In recent years, 1D-CNN has shown promising results in fault detection and diagnosis. Chen et al. extended the application of 1D-CNN based on one-dimensional process signals in complex multivariable process control and used reinforcement learning to search and optimize the structure of the neural network (Chen et al., 2022). Wu et al. developed an adversarial adaptive 1D-CNN that achieves high accuracy under different operating conditions (Wu et al., 2022). Wang et al. introduced batch normalization and improved second-order pooling into 1D-CNN, and used a multilayer perceptron for feature extraction and compression, which accelerated the convergence speed of the network (Wang et al., 2021).

However, the current approach to fault diagnosis tends to treat the entire process as an end-to-end classification task, where fault diagnosis is viewed as a multi-class classification problem. Historical process data is used to build a fault diagnosis model for the entire chemical process, and all faults are diagnosed using the same features and model. While this approach reduces manual intervention, it also has some drawbacks. For chemical processes, adopting such a fault diagnosis approach disregards the inherent mechanistic characteristics of the chemical process. Although it is challenging to establish an analytical model-based fault diagnosis model for the entire chemical process, it is feasible to adopt mechanism modeling for specific process units within the chemical process. On the other hand, for complex chemical processes, a single model is inability to perform effective feature extraction. Modeling different process units separately can better extract local features. Moreover, based on current results, deep learning networks also have certain limitations. If the network structure is too simple, the feature extraction capability is insufficient, leading to underfitting. On the other hand, deepening the network to extract features can easily result in overfitting. Directly modeling the entire chemical process is prone to these situations, which can lead to a decrease in the diagnosis performance of the network.

To solve the above problems, a novel fault diagnosis method named triage-based convolutional neural network (TrCNN) for fault diagnosis is proposed. The triage-based fault diagnosis method focuses on both the similarities and differences between faults. It is feasible to employ mechanism modeling for specific process units or to model different process units separately within the chemical process. Firstly, based on

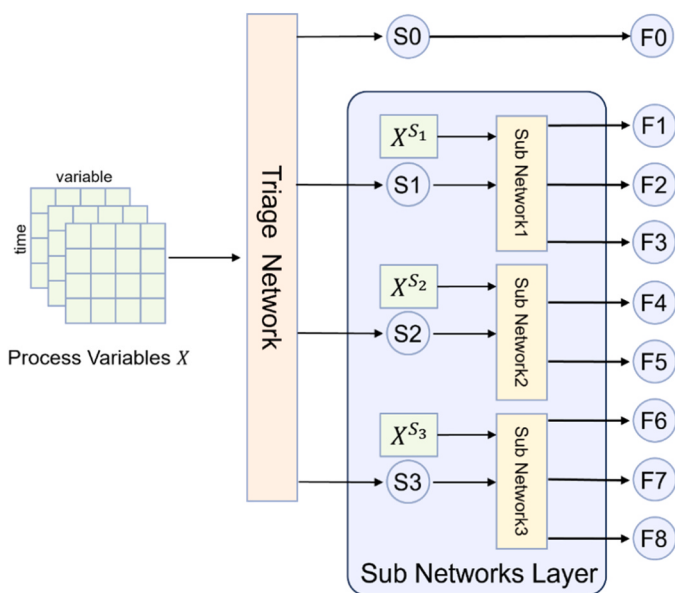


Fig. 1. The triage-based fault diagnosis architecture.

prior knowledge and certain rules, similar types of faults are grouped into a triage type, which can be linked to hospital departments. The specific types of faults can be considered as the causes determined through diagnosis. During the diagnosis process, the triage type, to which the fault belongs is determined, and then the specific fault category is diagnosed using the corresponding model. Through the implementation of triage-based approach, appropriate fault diagnosis models can be selectively applied to different units within the chemical process, effectively reducing the complexity of each task and enhancing the accuracy of diagnosis. This enables each model to individually build suitable feature models for the corresponding faults. Furthermore, for tasks of different stages and categories, feature selection using random forest is employed to eliminate weakly correlated features, enhance interpretability, and reduce unnecessary computation. Due to the excellent performance of 1D-CNN in extracting local features along the time dimension, it is chosen as the model structure in this paper. To better extract features along the time dimension, the data is transformed into a 2D time series matrix before conducting feature extraction along the time dimension.

The organization of the rest of this paper is as follows: In Section 2, the structure of triage fault diagnosis, fundamental theories about CNN, and CNN components are described in detail. Section 3 introduces the structure of TrCNN. In Section 4, the proposed method is applied on the TE process, and some insights into the model structure and performance are discussed. Finally, Section 5 concludes the paper.

2. Preliminaries

2.1. Triage fault diagnosis

In this study, a novel triage fault diagnosis (TFD) method for chemical processes is proposed. The faults are divided into different sets based on certain rules, with each set being assigned to a specific triage type. Each fault set can be trained and modeled using different strategies, including mechanism-based or data-driven approaches. During the modeling process, only the training dataset belonging to the respective triage type is utilized. Certainly, there needs to be a model responsible for global coordination among the triage types and determine which

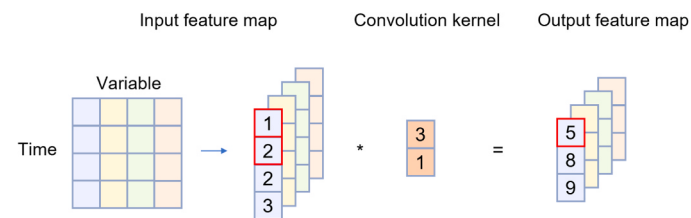


Fig. 2. Convolutional layer.

triage type the given data belongs to. This model is referred to as the triage network. The models responsible for diagnosing the specific fault type within each triage type are referred to as sub networks. By combining the triage network and sub networks for fault diagnosis, the location of the fault can be determined more quickly and accurately, enabling prompt actions to be taken to resolve the issue.

Fig. 1 illustrates the typical structure of TFD. It consists of two layers of networks. The first layer, known as the triage layer, utilizes the triage network to initially identify which triage type the process variables belong to. The second layer comprises several independent sub networks, with each sub network dedicated to refining the specific fault types within the triage types identified in the first layer, ultimately diagnosing the specific fault types. The triage layer classifies the input X into d triage types denoted as $[S_0, S_1, \dots, S_{d-1}]$, where $i=0$ represents the normal operating condition. The second layer consists of $d-1$ sub networks $[SN_1, SN_2, \dots, SN_{d-1}]$ corresponding to the triage types S_1 to S_{d-1} . Each sub network SN_i identifies its sub-state based on the input X^S_i . As the normal operating state has only one category, it is directly identified by the triage network without requiring the sub networks for diagnosis.

2.2. Convolutional neural network

CNN is a deep learning model that was initially proposed in the late 1980 s (Cun et al., 1989). Its core ideas include local connectivity, weight sharing, pooling, and the use of multiple layers (LeCun et al., 2015). 1D-CNN is a variant of CNNs that is primarily used for processing one-dimensional sequence data such as text and audio data. The basic structure of a 1D-CNN is similar to traditional CNNs and includes convolutional layers, pooling layers, fully connected layers, and activation functions. The key difference between 1D-CNN and traditional CNN lies in the operation of the convolutional kernel. In 1D-CNN, the convolutional kernel slides in only one direction, typically along the time axis. This allows the 1D-CNN to extract temporal features from the data and share the same convolutional kernel across different positions.

For multivariate time series data, the order of variables does not necessarily follow a specific sequence. Therefore, it is only possible to assume local pattern invariance along the time dimension, unlike images that have both horizontal and vertical dimensions (Zhang and Qiu, 2022a). Consequently, using 1D-CNN for processing multivariate time series data is appropriate.

2.2.1. Convolutional layer

The convolutional layer, also known as the feature extraction layer, is used to process multivariate time series data. In 1D-CNN, the data is stacked as a two-dimensional matrix, where each vector represents the time series values of a specific process variable. Each variable is treated as a separate channel, and convolution is performed along the time dimension. The output feature maps are obtained by applying convolutional operations to the input features. Fig. 2 illustrates the convolutional computation process of 1D-CNN on a time series. When the input data is 4×4 , 1D-CNN stacks the four variables and performs

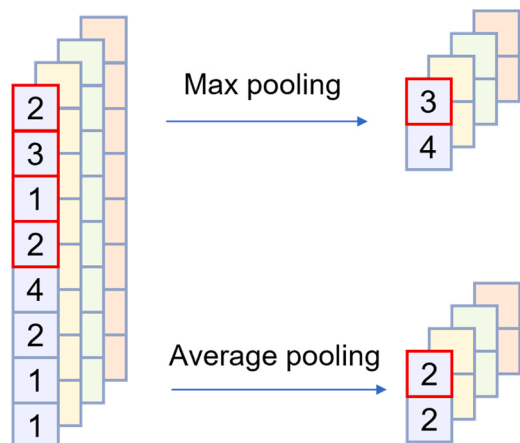


Fig. 3. Pooling layer.

feature extraction by sliding the convolutional kernel along the time dimension. In the figure, the convolutional kernel has a size of 2 and a stride of 1.

After the convolutional operation, it is common to include a bias term and apply an activation function to introduce non-linearity in the network. Activation functions that are commonly used include the logistic function(sigmoid), hyperbolic tangent function(tanh), and rectified linear unit (ReLU).

$$f(x) = (1 + e^{-x})^{-1} \quad (1)$$

$$f(x) = \tanh(x) \quad (2)$$

$$f(x) = \max(0, x) \quad (3)$$

2.2.2. Pooling layer

The pooling layer is a type of layer that performs down sampling on the data. It is used to reduce the dimensionality of the feature maps obtained from the convolutional layer and retain important information, thus reducing the complexity of the model and improving its generalization ability. In the pooling layer, commonly used pooling operations

include max pooling and average pooling, as shown in Fig. 3.

2.2.3. Fully connected layer

After multiple layers of convolution and pooling operations, the features have been extracted. The goal of the fully connected layer is to classify the extracted features. All the feature maps outputted from the previous layer are flattened into a one-dimensional vector and then fed into the fully connected layer. The fully connected layer outputs a set of scalar values.

3. System structure of triage fault diagnosis

In chemical processes, faults occur when process variables deviate from their normal states, and the underlying causes may be related to only a few variables. The data of different deviations can be used for diagnosing fault types. However, faults in chemical processes often exhibit similarities. For example, the fault behavior of a step change in reactor cooling water inlet temperature and a random variation in reactor cooling water inlet temperature may have significant similarities. In the process of fault diagnosis, it is not always necessary to determine the specific fault type that occurred. It can be sufficient to identify two or several highly probable faults. Additionally, due to the high similarity between some faults, it may be difficult to directly differentiate all fault types using a single model. Therefore, it is possible to first diagnose the range to which a fault belongs, known as the triage type in this paper, and then use a more refined model to determine the specific fault type.

The fault diagnosis model for the chemical process based on the triage-based CNN extracts features from a period of process data and diagnoses the system state. The model takes a 2D vector of size $m \times n$ as input, where m is the number of features and n is the length of the time series. The model outputs the triage type (including normal operation) and the specific fault type.

The framework of the TFD is shown in Fig. 4. The method is mainly divided into two parts: offline process fault diagnosis and online process fault diagnosis. The details of the algorithm are described in the following sections.

Algorithm 1. Fault diagnosis based on triage-based convolutional neural network.

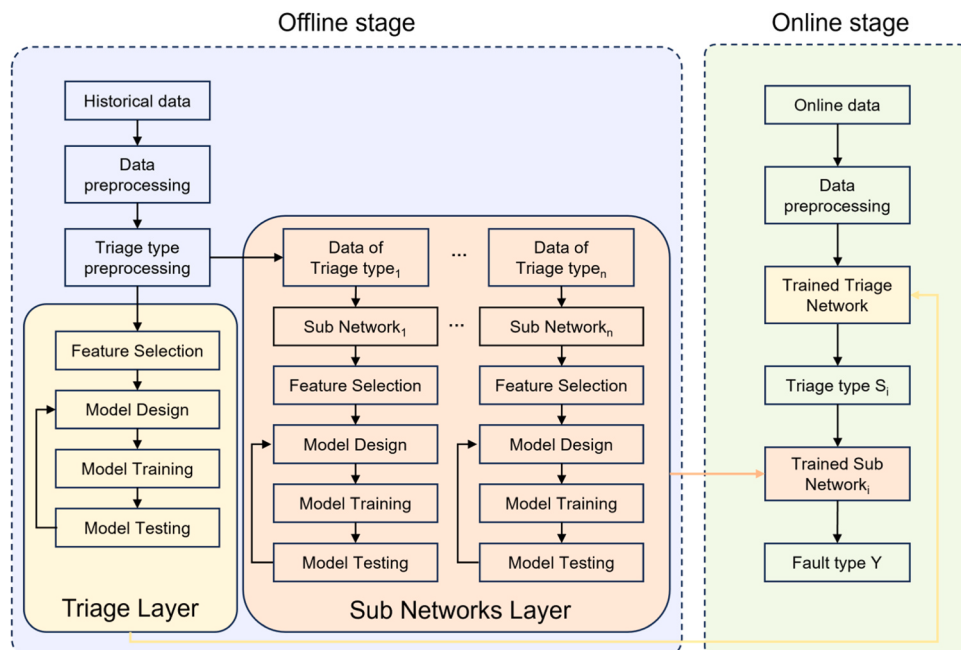


Fig. 4. The framework of triage-based fault diagnosis method.

Offline Stage:

Step 1: Historical process data (X, Y) is collected and divided into train set (X_{train}, Y_{train}) and test set (X_{test}, Y_{test}) .

Step 2: Through data preprocessing, raw data is standardized and transformed into $m \times n$ samples.

Step 3: The triage type S to which the fault type Y belongs is determined based on prior knowledge and rules.

Step 4: Features are selected based on their contribution using the random forest algorithm.

Repeat:

Step 5: The triage network and the sub networks are designed for the chemical process.

Step 6: The triage network is trained with (X_{train}, S_{train}) and each sub network SN_i is trained with $(X_{train}^{S_i}, Y_{train})$.

Step 7: The networks are tested with the test set and judged by FDR and FPR.

Until:

The testing FDR and FPR are satisfactory.

Online stage:

Step 1: Online data X is collected from a chemical process.

Step 2: Preprocessing is applied to transform online data into samples of size $m \times n$.

Step 3: According to eq 4, the online data is passed through the triage layer, providing a prediction for the triage type.

$$S_i = TriageNetwork(X) \quad (4)$$

Step 4: According to eq 5, based on the predicted triage type, the corresponding sub network is used for diagnosis, providing a prediction for the specific fault type.

$$Y = SubNetwork_i(X^{S_i}) \quad (5)$$

In this algorithm, the fault detection rate (FDR) and false positive rate (FPR) are commonly used to evaluate the fault diagnosis performance. They are calculated using Eq. 6 and Eq. 7 respectively, where TP, FP, TN, and FN are determined based on the confusion matrix, as detailed in Table 1.

$$FDR = \frac{TP}{TP + FN} \quad (6)$$

$$FPR = \frac{FP}{FP + TN} \quad (7)$$

4. Case study on tennessee eastman process

4.1. TE data and preprocessing

The TE process is a computer simulation process based on real chemical process data, designed by Downs and Vogel (Downs and Vogel, 1993). To enhance the applicability of this model, Bathelt et al. proposed a modified version of the TE process (see Fig. 5) and expanded the variables (Bathelt et al., 2015). The modified version can be obtained from <http://depts.washington.edu/control/LARRY/TE/download.html>. The benchmark TE process was utilized to verify the effectiveness of the proposed TrCNN model in this study.

Table 1
Confusion Matrix.

Confusion Matrix		Prediction Positive	Negative
Real	Positive	TP	FN
	Negative	FP	TN

In the simulation, a total of 53 variables were considered, comprising 12 process manipulation variables, 22 continuous process measurements, and 19 composition analysis measurements. Notably, the compressor recycle valve (5), stripper flow valve (9), and reactor agitator rate (12) maintained constant values. Consequently, the dimension of the process data utilized in subsequent model training was reduced to 50. For the evaluation of model performance, 15 fault types represented by IDV1 - IDV15, along with the normal state IDV0, were selected. Faults 16–20 were excluded from the study due to uncertain fault types. The sampling period was set at 3 min, equivalent to 20 points per hour. During simulations of normal operating conditions, the system's initial conditions were altered for each simulation. Ten simulations were conducted under each condition, each lasting for 50 h, resulting in a total of 10,000 data samples under normal conditions. For training purposes, 80% (8000) of the normal condition data were randomly selected as the training set, while the remaining 20% (2000) were reserved as the test set. In simulating fault conditions, 10 simulations were performed under different initial conditions. It is noteworthy that we initiated simulations with 10 h of normal state to ensure system stability. Subsequently, fault disturbances were introduced, and simulations were extended for an additional 40 h to obtain data under fault conditions. However, for fault 6 (IDV6), the simulation was terminated after 7 h due to the system's reaction pressure exceeding the limit, triggering a shutdown. Similarly, for each fault, 8 simulated fault samples were randomly chosen (from a pool of 90,720) as the training set, and 2 simulated fault samples were designated as the test set. A detailed overview of the simulation information is presented in Table 2.

4.2. Implementation details

Variable selection is closely related to the fault diagnosis model performance. The complete dataset comprises 50 features. However, not all features are effective, given that an excess of variables can lead to a waste of computational resources, particularly in the context of deep learning. Whether a variable is valuable or noise is determined by the model performance that if it is improved or on the contrary. RF, a common embedded feature selection method, is relatively easy to understand and implement (Chen et al., 2020; Kari et al., 2023). For TrCNN, the identification of key variables relevant to different faults varies. Utilizing the feature importance ranking computed by RF, 35 features were retained for both the triage layer model and the sub networks layer model.

4.2.1. Triage layer

In the event of a malfunction, timely and effective diagnosis is crucial for identifying the root cause of the problem and implementing appropriate measures for resolution. The triage layer is capable of quickly distinguishing whether the current operating condition is abnormal and can provide possible causes for the malfunction. Additionally, since the subnetwork layer relies on the diagnostic effectiveness of the triage layer model, the triage layer is also crucial for the overall diagnostic performance. In this study, the performance of the triage layer was investigated under different triage approaches to present enhanced solutions for chemical process fault diagnosis.

Two triage approaches were considered: based on the occurrence location of faults and based on the fault types. Triage based on location of faults categorizes faults occurring at the same location into one category. The TE process can be categorized into four categories based on the location of the fault: reactor feed, reactor, condenser, and stream 4. Furthermore, the faults can be classified into five categories based on their types: material temperature faults, feed composition faults, valve faults, cooling water inlet temperature faults, and other faults. The

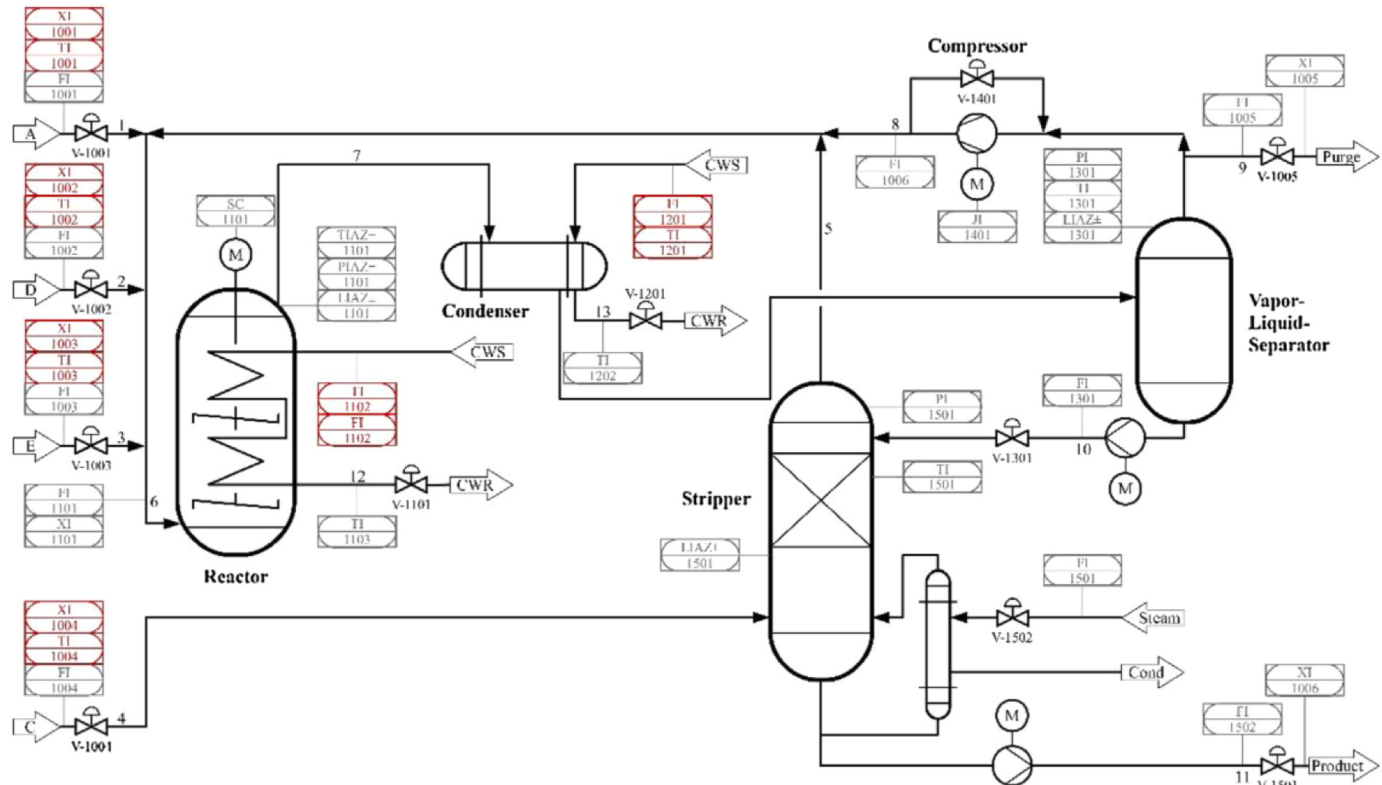


Fig. 5. Revised TE process (Bathelt et al., 2015).

Table 2

Simulation Time and Sample Size of Each Status.

Status	Training Set simulation time/h	Testing Set simulation time/h	Training Set sample size	Testing Set sample size
Normal	$50 \times 10 \times 0.8$	$50 \times 10 \times 0.2$	8000	2000
IDV 01-05 07-15	$40 \times 10 \times 14 \times 0.8$	$40 \times 10 \times 14 \times 0.2$	89600	22400
IDV 06	$7 \times 10 \times 0.8$	$7 \times 10 \times 0.2$	1120	280
Total	4936	1234	98720	24680

Table 3

Triage Approaches of the TE Process.

Triage approach	Faults type	Triage type
Fault location	Fault 3, Fault 6, Fault 9 Fault 4, Fault 11, Fault 13, Fault 14 Fault 5, Fault 12, Fault 15 Fault 1, Fault 2, Fault 7, Fault 8, Fault 10	Feed of reactor Reactor Condenser Stream 4
Fault type	Fault 3, Fault 9, Fault 10 Fault 1, Fault 2, Fault 8 Fault 14, Fault 15 Fault 4, Fault 5, Fault 11, Fault 12 Fault 6, Fault 7, Fault 13	Material temperature faults Feed composition faults Valve faults Cooling water inlet temperature faults Other faults

specific triage approaches are presented in [Table 3](#). Additionally, regardless of the triage approach employed, the normal operating condition is treated as a separate triage category to facilitate the timely detection of abnormal operating conditions at the triage layer.

When diagnosing in the triage layer, it is not necessary to accurately determine the specific type of the fault. It is only necessary to diagnose the triage category to which it belongs. Therefore, overly complex models can lead to overfitting and a decrease in the actual diagnostic performance. To achieve maximum computational efficiency in training and classification, several simple 1D-CNN network models were developed and tested, as shown in [Table 4](#). To determine the optimal triage layer, 25% of the training set were randomly selected as the validation set, while the remaining 75% were reserved as the training set. The validation set was used to assess the model's performance and select an appropriate triage model and approach. The network model with the most outstanding diagnostic performance on validation set from [Table 4](#) was selected as the architecture for the triage task. Taking Model 1 as an example, the structure of the models in [Table 4](#) is explained. In this instance, the model comprises three layers, including one 1D convolutional layer, one max pooling layer, and one fully connected layer. The convolutional layer has a kernel size of 5, a stride of 1, and a padding of 2 to ensure that the size of the output feature map remains the same as the input data during convolution. There are 32 convolutional kernels. The pooling layer utilized max pooling has a kernel size of 2 and a stride of 2. The input to the fully connected layer must be a one-dimensional vector, so the Flatten operation is employed to reshape the 2D array into 320 (10×32). The output of the fully connected layer is obtained using softmax to acquire the final prediction. The experimental optimizer is Adam, and the activation function is ReLU.

4.2.2. Sub networks layer

Different tasks require different neural network architectures. In the case of the sub network layer, it is often necessary to use multiple neural networks to diagnose different types of faults separately, to accurately identify the specific fault. These sub networks can have different network structures, with each sub network trained and adjusted

Table 4

Model Candidates for Fault Diagnosis of the TE Process.

Model	Architecture
Model 1	Conv(32)-Pool-FC(16)
Model 2	Conv(32)-Pool-Conv(64)-Pool-FC(16)
Model 3	Conv(32)-Conv(64)-Pool-FC(16)
Model 4	Conv(32)-Conv(64)-Pool-Conv(64)-Pool-FC(16)
Model 5	Conv(64)-Pool-FC(128)-FC(16)
Model 6	Conv(128)-Pool-FC(16)

Table 5

The Training Time and the Average FDR of Validation Set.

Triage approach	Model	Training time for one epoch (s)	Validation set average FDR (%)
Fault location	Model1	2.27	97.5
	Model2	2.82	94.7
	Model3	3.00	96.7
	Model4	3.52	95.7
	Model5	2.70	97.0
	Model6	2.31	97.1
	Model1	2.09	92.1
	Model2	2.74	91.0
	Model3	2.70	90.6
	Model4	3.29	90.0
	Model5	2.41	91.2
	Model6	2.17	91.2

specifically for a particular type of fault, to better capture the features of these faults. Designing an optimal network structure without scientific guidance can be a complex task.

To identify suitable models, the Particle Swarm Optimization (PSO) algorithm was employed to explore appropriate network structures and automatically optimize the training process and parameters. Through this optimization, suitable sub networks for each triage type were determined. In this study, different choices for the convolutional kernel size were considered, including 3×1 , 5×1 , and 7×1 . The number of convolutional layers ranged from 2 to 6, and the pooling layer utilized max pooling with a constant kernel size of 2 and a stride of 2. The learning rate was selected within the range of 10^{-2} to 10^{-5} .

4.3. Results and discussion

The training and testing processes were conducted on a server with a 3090 GPU. The batch size for the training set was set to 128, meaning that the samples were input into the model in small batches. During each iteration, 128 samples were used for forward and backward propagation. The training was performed for 50 epochs, meaning that the training dataset was iterated 50 times for model training. To prevent overfitting, an early stopping strategy was employed.

4.3.1. Triage layer diagnosis result

[Table 5](#) presents the average FDR of validation set and training time for different triage approaches (as shown in [Table 3](#)) and model structures (as shown in [Table 4](#)). Among the triage approaches, using fault position to determine the triage category and training with Model 1 achieves the highest average FDR (97.5%) and requires shorter training time. In the subsequent discussion, the triage layer adopts the triage method based on fault position and Model 1 is selected as the optimal architecture.

After determining the triage approach and network structures including hyperparameters of triage layer, all training set including validation set were used to train the model and the test set was used to verify the model performance. [Fig. 6](#) illustrates the accuracy curves during the training and testing phases of triage network. For the testing dataset containing 24,680 data points, the triage layer successfully classifies them into five different triage types, including the normal

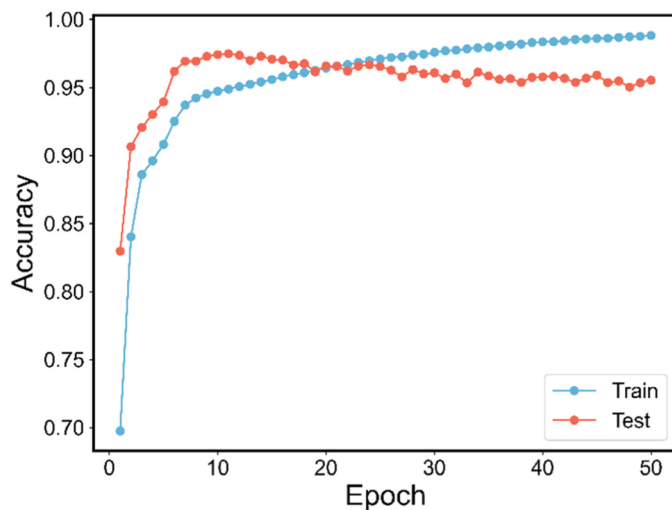


Fig. 6. Training and testing accuracy with the epoch of triage network.

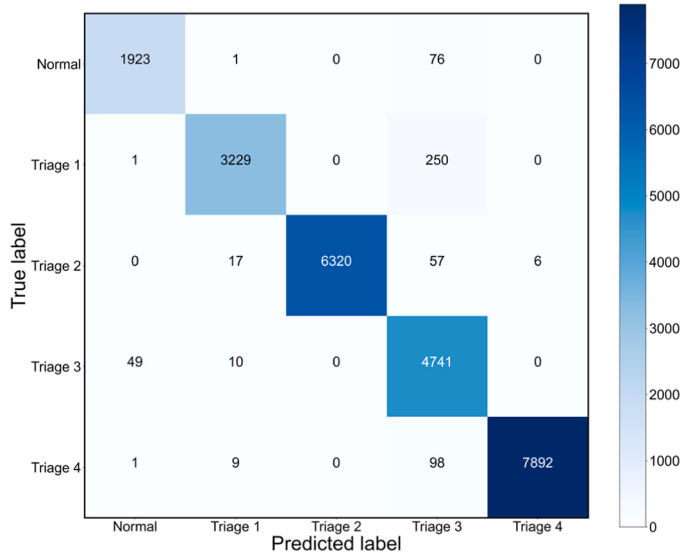


Fig. 7. Triage layer confusion matrix for the testing set.

condition. The confusion matrix of the triage layer's diagnostic results is shown in Fig. 7, where the numbers on the main diagonal represent the correctly identified samples. It can be observed that the triage layer achieves overall good diagnostic performance when based on fault position for triaging.

4.3.2. Sub networks diagnosis result

Triage based on fault position results in five triage types: reactor feed, reactor, condenser, stream 4, and normal condition. Since the normal condition is already diagnosed in the triage layer and does not require further diagnosis, there are four sub networks dedicated to diagnosing faults. Each sub network focuses on diagnosing specific types of faults.

For different triage categories, the sub network layers identify the top 5 variables with the highest contribution through the random forest algorithm, as shown in Table 6. It can be observed that different sub networks within the layer retain variables that are correlated with the respective triage categories when diagnosing specific faults. For instance, in diagnosing faults belong to feed of reactor, the variables with the highest impact include flow indicators at the feed of reactor and indicators of reactor condenser water.

Table 6

Top 5 variables of different triage types.

Triage type	Top 5 variables with the largest random forest score
Feed of reactor	XMEAS (21) Reactor cooling outlet temp. XMEAS (1) A feed rate XMV (3) Valve pos. A feed XMV (11) Valve pos. condenser cooling water XMEAS (22) Separator cooling outlet temp.
Reactor	XMV (11) Valve pos. reactor cooling water XMEAS (21) Reactor cooling outlet temp. XMEAS (9) Reactor temp. XMEAS (24) Reactor feed B% XMEAS (18) Purge temp.
Condenser	XMEAS (18) Purge temp. XMV (11) Valve pos. condenser cooling water XMEAS (11) Separator temp. XMV (2) Valve pos. E feed XMV (8) Valve purge pos. stripper steam
Stream 4	XMV (4) Valve pos. A&C feed (stream 4), XMV (3) Valve pos. A feed (stream 1) XMEAS (34) Purge gas F% XMEAS (28) Reactor feed F% XMEAS (24) Reactor Feed B%

Table 7

Diagnosis Result of the Sub Networks.

Triage type	Fault type	Testing average FDR (%)
Feed of reactor	Fault3 D feed temperature increases	97.2
	Fault6 A feed loss	99.3
	Fault9 D feed temperature changes randomly	96.7
	Fault4 reactor cooling inlet temperature increases	99.9
	Fault11 reactor cooling water inlet temperature changes randomly	99.4
	Fault13 reaction kinetics drift slowly	100
	Fault14 reactor cooling water valve sticking	99.8
	Fault5 condenser cooling inlet temperature increases	94.9
	Fault12 condenser cooling inlet temperature changes randomly	97.1
	Fault15 condenser cooling water valve sticking	97.5
Reactor	Fault1 A/C feed ratio decreases (A&C feed)	99.8
	Fault2 B composition increases (A&C feed)	99.4
	Fault7 C feed header pressure loss-reduced availability	100
	Fault8 A, B, and C feed composition changes randomly	98.7
	Fault10 C feed temperature changes randomly	99.3
Condenser	Fault1 A/C feed ratio decreases (A&C feed)	99.8
	Fault2 B composition increases (A&C feed)	99.4
	Fault7 C feed header pressure loss-reduced availability	100
	Fault8 A, B, and C feed composition changes randomly	98.7
	Fault10 C feed temperature changes randomly	99.3
Stream 4	Fault1 A/C feed ratio decreases (A&C feed)	99.8
	Fault2 B composition increases (A&C feed)	99.4
	Fault7 C feed header pressure loss-reduced availability	100
	Fault8 A, B, and C feed composition changes randomly	98.7
	Fault10 C feed temperature changes randomly	99.3

The diagnostic results of each model are presented in Table 7, indicating high diagnostic performance for specific faults within their respective triage types, where the network structure optimised by the particle swarm algorithm for different shunt types in the sub-network layer is shown in Table S1. To further analyze the diagnostic results, the confusion matrices for different sub networks are shown in Fig. 8. The matrices display the diagnostic outcomes for various faults within different triage types. It can be observed that the diagnostic rates for faults 5, 12, and 15 in triage type 3 are slightly lower compared to other types. This may be attributed to the fact that these faults all occur in the condenser location and have similar fault patterns. Faults 5 and 12 involve variations in the temperature of condenser inlet water, while fault 15 is related to the sticking of the cooling water valve, resulting in a similar effect of temperature change. Overall, it can be concluded that the different models perform well in diagnosing specific faults within their corresponding triage types, indicating the effectiveness of the triage approach.

To visually illustrate the recognition performance of various models in the sub network layer for specific fault states within their respective triage types, the t-distributed stochastic neighbor embedding (t-SNE) method was utilized. The t-SNE algorithm effectively reduces high-dimensional data from the intermediate layers of the network into two-dimensional or three-dimensional space, facilitating the visualization of the output from the intermediate layers of the model.

t-SNE graphs were generated for the features extracted from the sub

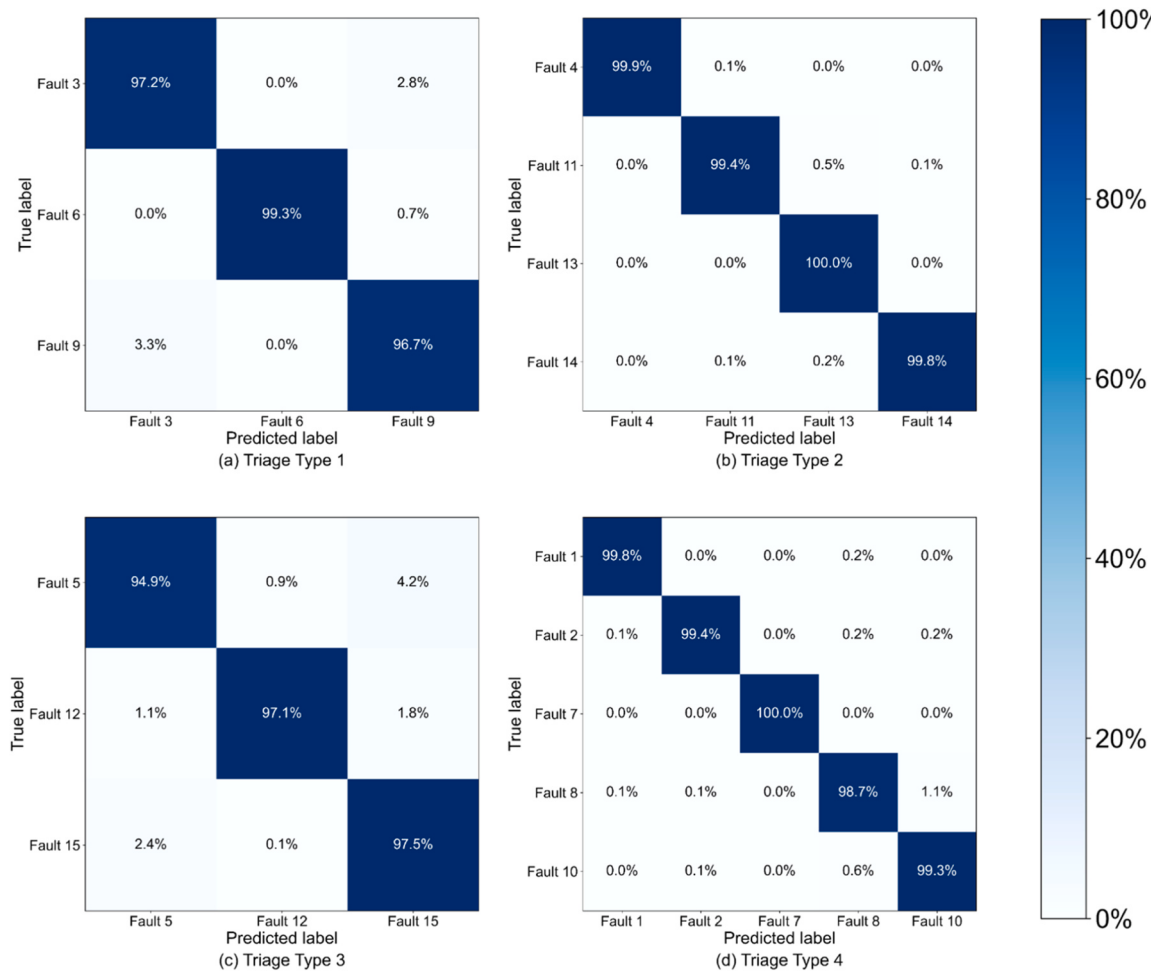


Fig. 8. Sub networks layer confusion matrix for the testing set.

network layer models employing convolutional neural networks. For each triage type, a random selection of 1000 samples from the dataset were visualized. As shown in Fig. 9, it can be observed that after the extraction by 1D-CNN, there is a clear clustering trend, and the clustering results can also distinguish different types of faults. Most of the fault types can be well classified, with only a few overlaps. This indicates that the feature extraction through the convolutional layers is effective and can be used successfully to differentiate specific fault types.

4.3.3. Triage-based Diagnosis Result

After the structures of the triage layer and sub networks layer were determined, the overall performance of the fault diagnosis based on the triage-based model was tested. The diagnostic results are shown in Table 8. As shown in the table, the average FDR for the training set is 97.69%, with a corresponding FPR of 0.16%. For the testing set, the average FDR and FPR are 96.78% and 0.22% respectively. The results indicate that, except for fault 5 (step change in condenser cooling water inlet temperature) and fault 9 (random variation in temperature of stream 2 component D), the diagnosis rates of our method are all above 96%, with fault 15 having a slightly higher FPR but still below 3%. It can be observed that the performance of the training set and testing set data is close, indicating that the model does not exhibit significant overfitting. Overall, the TrCNN model is capable of accurately identifying these types of faults.

To further explore the diagnostic results, the confusion matrix for the overall diagnosis results was plotted as shown in Fig. 10. The confusion matrix reveals that the primary fault prone to misdiagnosis is fault 9 (associated with triage type 1), often incorrectly diagnosed as fault 15

(associated with triage type 3). Fault 9 and fault 15 belong to different triage types, indicating an error during the triage stage where fault 9 of triage type 1 is misdiagnosed as fault 15 of triage type 3. To enhance the diagnostic accuracy of fault 9 in the future, optimization of the triage layer can be considered.

Fig. 11 shows the diagnostic probabilities of the model for the first 3 h after the occurrence of fault 1. In the early stages of fault occurrence, fault 1 is prone to be misdiagnosed as fault 15 and fault 9. However, after 15 min, it can be accurately identified. Furthermore, the diagnostic rates of all fault types in the early stages of fault occurrence were statistically analyzed and are presented in Table 9. The results show that although the average FDR in the first hour only reaches 54%, there is significant improvement between 1 to 2 h, with an FDR exceeding 90%. This indicates that the model provides timely diagnosis. In future research, it is necessary to focus on ultra-early warning for faults, particularly in improving the fault detection effectiveness within the first hour.

To enhance the understanding of the feature learning process in the triage-based 1D-CNN model, the t-SNE method was utilized to visualize the outputs of each layer in the network. Fig. 12 illustrates the progressive changes of 5000 randomly selected test samples in the triage network. All different categories of raw data are mixed, making it difficult to distinguish. However, after being extracted by the model, the samples gradually cluster in the t-SNE plot, showing clear clustering effects. However, after feature extraction by the model, the samples gradually cluster in the t-SNE plots, demonstrating evident clustering effects.

For the sub networks layer, Fig. 13 presents the t-SNE visualization of

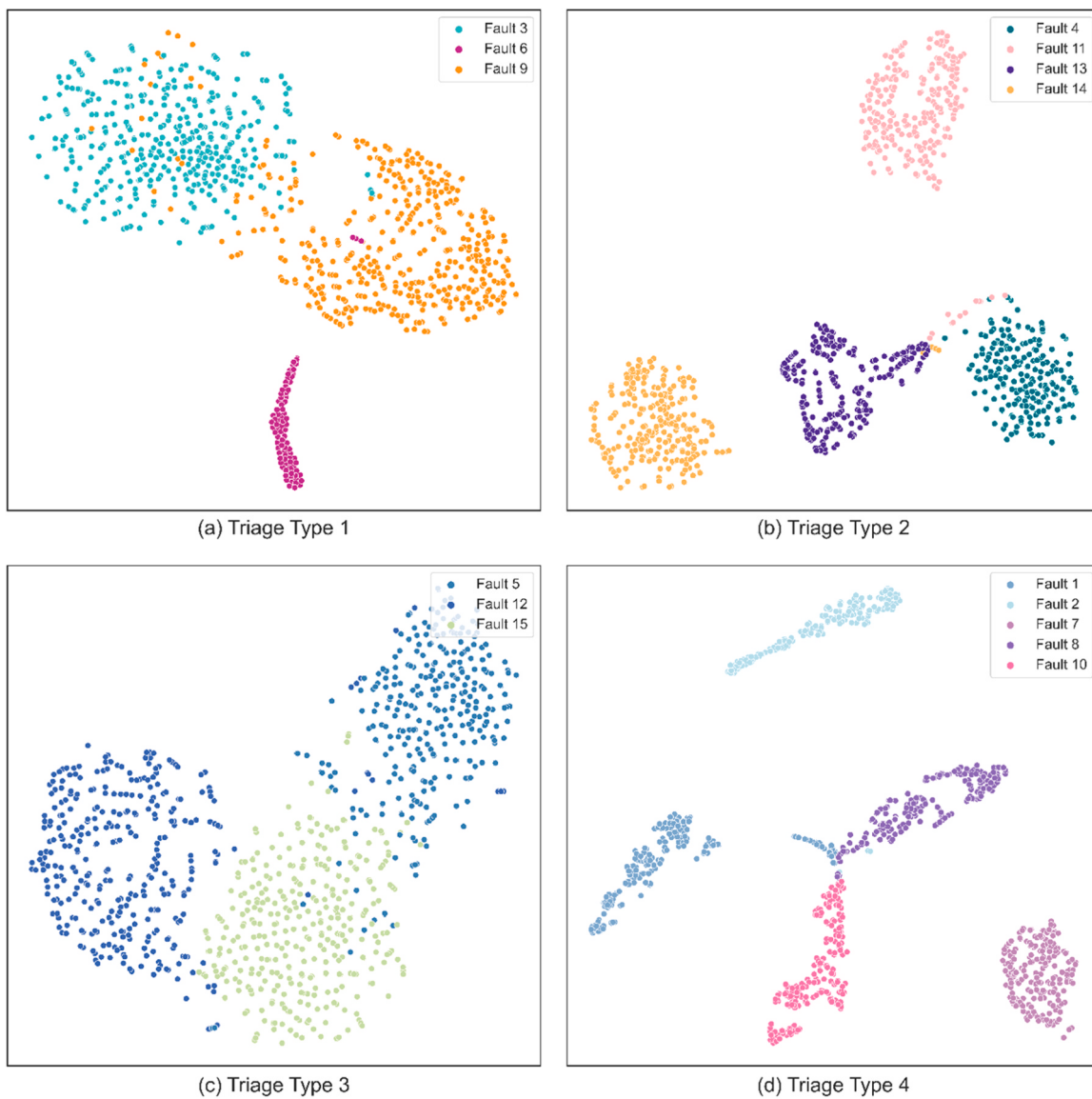


Fig. 9. Different models of sub networks visualization using t-SNE.

Table 8
Diagnosis Result of the TE process.

Type of fault	Fault diagnosis rate (FDR/%)		False positive rate (FPR/%)	
	Training Set	Test Set	Training Set	Test Set
Fault 1	99.83	99.63	0.00	0.00
Fault 2	99.42	99.13	0.02	0.02
Fault 3	99.55	97.19	0.01	0.23
Fault 4	100.00	99.94	0.00	0.00
Fault 5	95.47	91.81	0.55	0.26
Fault 6	99.55	98.93	0.00	0.00
Fault 7	100.00	100.00	0.00	0.00
Fault 8	98.47	97.13	0.03	0.01
Fault 9	87.53	81.63	0.14	0.33
Fault 10	96.73	97.25	0.01	0.00
Fault 11	99.42	98.88	0.00	0.00
Fault 12	98.53	97.13	0.08	0.10
Fault 13	96.50	96.88	0.00	0.00
Fault 14	99.67	99.25	0.00	0.00
Fault 15	94.72	96.94	4.76	2.44
Average	97.69	96.78	0.37	0.23

each layer for the model corresponding to sub network layer triage type 1. It can be observed that in addition to faults 3, 6, and 9, which belong to triage type 1, a few faults from other categories are misdiagnosed as triage type 1. Fault 6 can be distinguished well from the beginning, while faults 3 and 9 are mixed and challenging to differentiate. As the model extracts features, the two categories gradually exhibit clustering tendencies and can eventually be effectively separated.

The diagnostic performance of DCNN, attention-BiLSTM, 1D CNN, TrCNN* (TrCNN without RF-based feature selection method) and TrCNN are presented in Fig. 14, while the specific results are shown in Table S2 and S3. The triage-based methods produced better FDR and FPR than DCNN, attention-BiLSTM, 1D CNN. The average FDR and FPR of TrCNN* improved after employing the RF-based feature selection method. This is because the triage network categorizes faults into multiple distinct types, and each type focuses on different key features. After feature selection, it retains the crucial features for each category, thereby assisting our network in achieving more precise diagnostics. In detail, our triage-based models performed much better for the diagnosis of faults 9 and 15. The FDR of fault 9 was 80.63% for TrCNN* and 81.63% for TrCNN, compared with only 61.38% for attention-BiLSTM and even 47.88% for attention-BiLSTM. The triage-based method

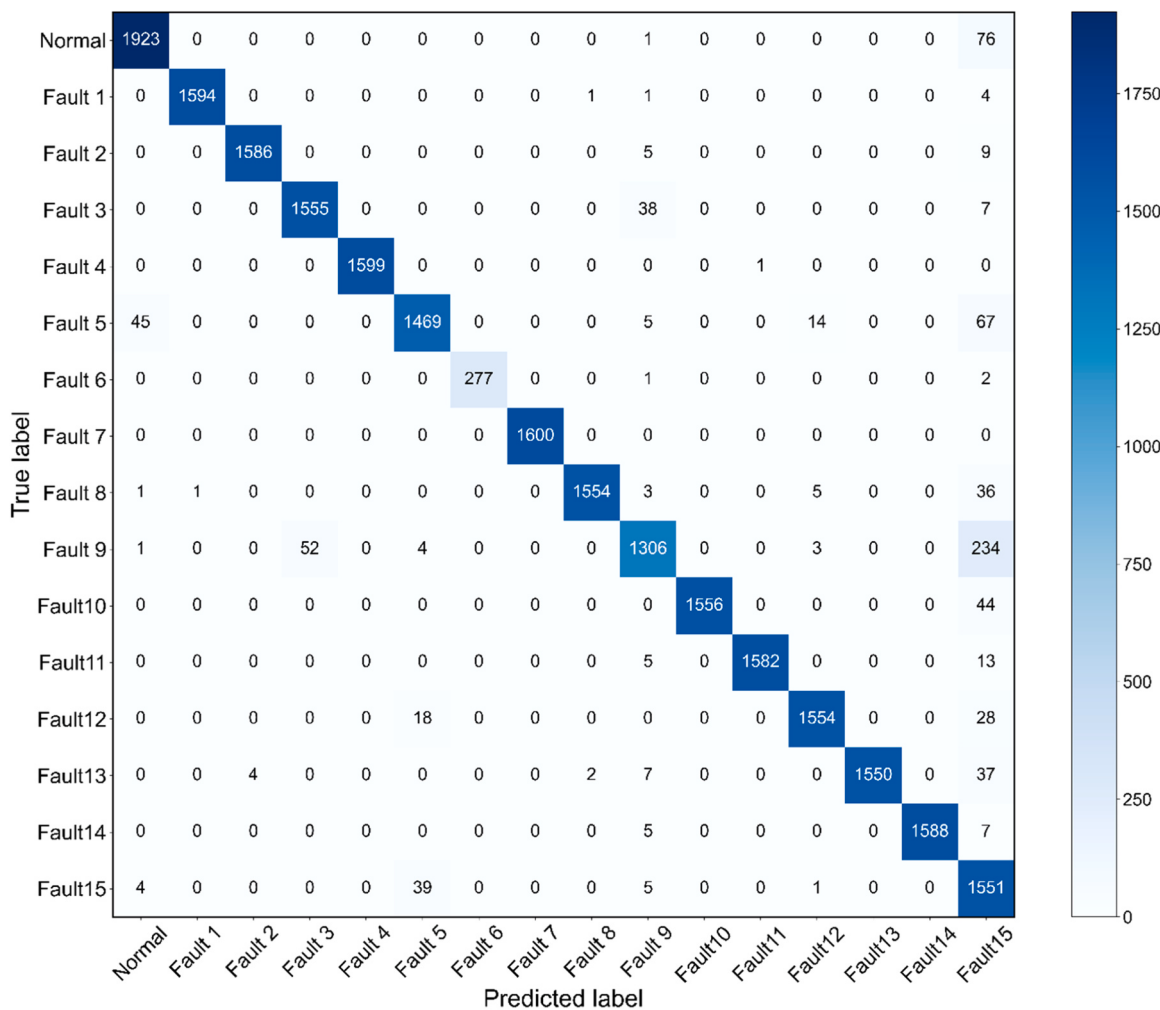


Fig. 10. Confusion matrix for testing set.

proves to be effective in diagnosing similar faults and is well-suited to serve as a fundamental framework for FDD. In addition, the FDRs of these five methods at different time periods after introducing faults are presented in Table S4. All methods exhibited low diagnosis rates in the initial hour after the occurrence of faults. Nevertheless, whether in the early stages of fault occurrence or in a certain period after the fault,

TrCNN consistently performed well.

The TrCNN first determines the triage type through the triage network and then identifies the specific fault type through the sub-networks. However, in chemical production processes, unknown types of faults which not included in the historical process data may occur. In the case of unknown faults, determining the specific fault type poses a

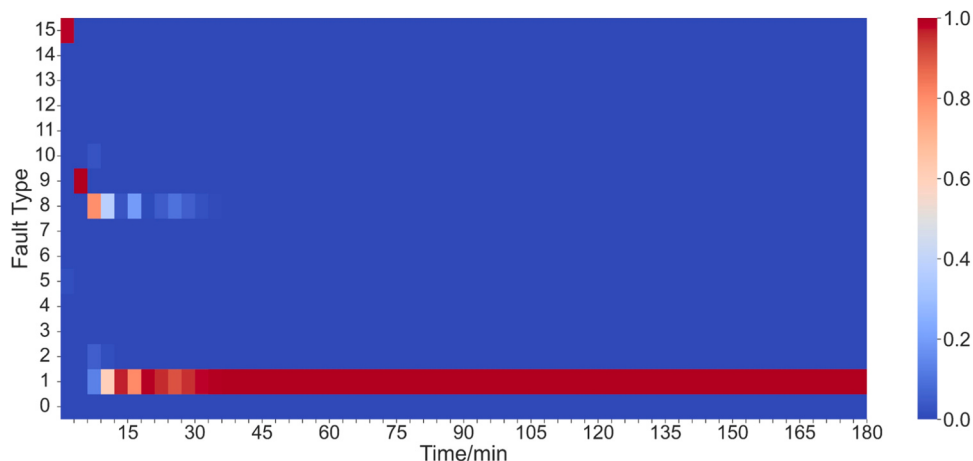


Fig. 11. Visualization of categorical probabilities in triage-based fault diagnosis after fault 1 has been introduced for 60, 120, and 180 min, respectively.

Table 9

The average FDR during different time period after the fault introduction.

Time period	0–1 h	1–2 h	2–3 h
Average FDR (%)	54.00	94.67	100.00

challenge. However, the triage network allows it to obtain the triage type. Specifically, when using the location of the fault occurrence as the triage category, the triage network can help identify the location of unknown faults, assisting personnel in narrowing down the troubleshooting scope. To evaluate the diagnosis performance of the proposed method for unknown fault types, experiments were conducted

separately for each of the selected faults: Fault 3 (Triage type 1), Fault 11 (Triage type 2), Fault 15 (Triage type 3), and Fault 2 (Triage type 4). During each experiment, only the other 14 known faults were considered, and the unknown fault type was introduced only during testing. The average FDR for each fault occurs when treated as an unknown fault is presented in the Table 10. It is evident that the proposed method can achieve reasonable diagnostic results even for unknown fault types, which is meaningful for the practical application of chemical process fault diagnosis in real production scenarios.

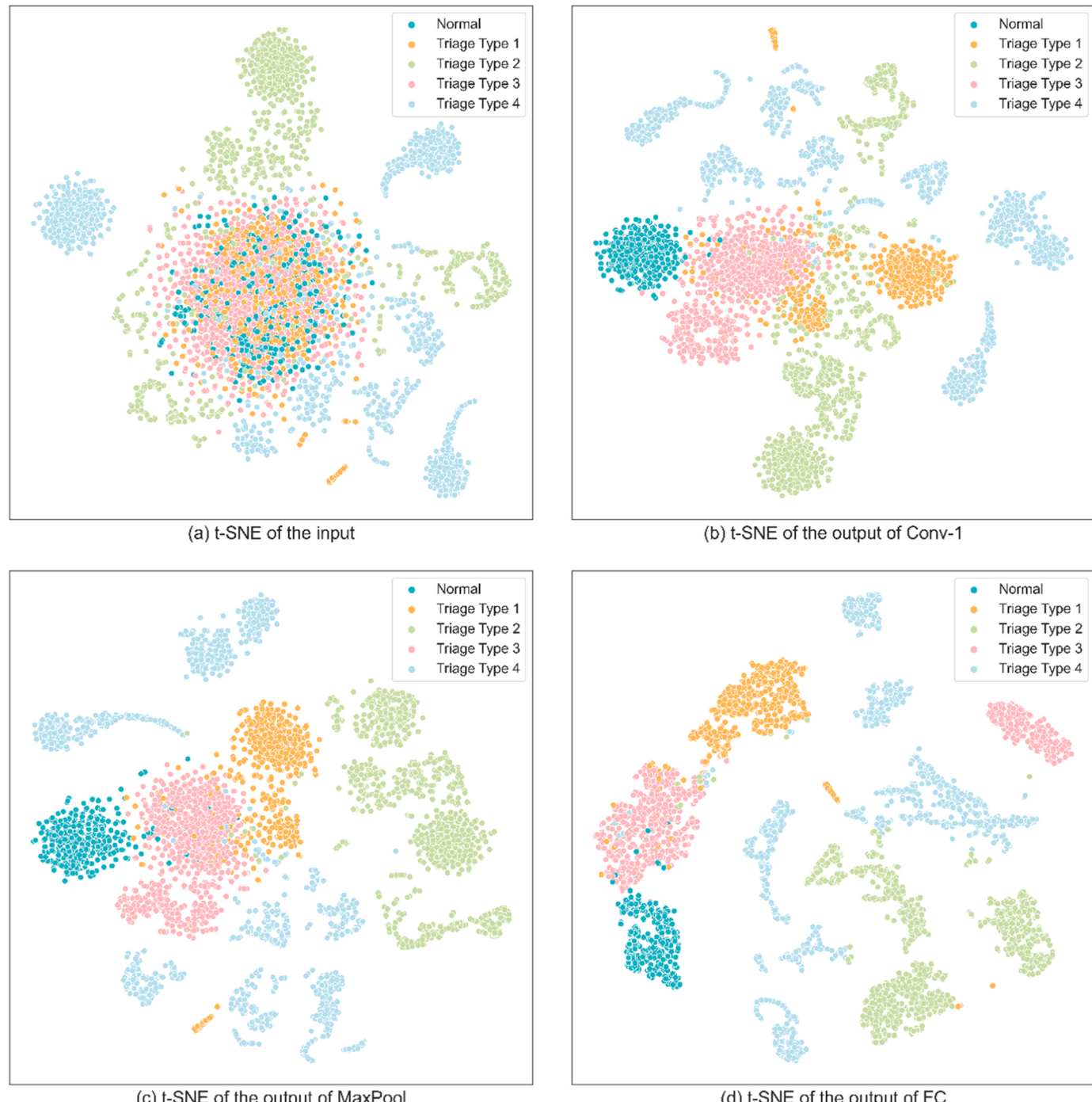


Fig. 12. Triage layer visualization using t-SNE.

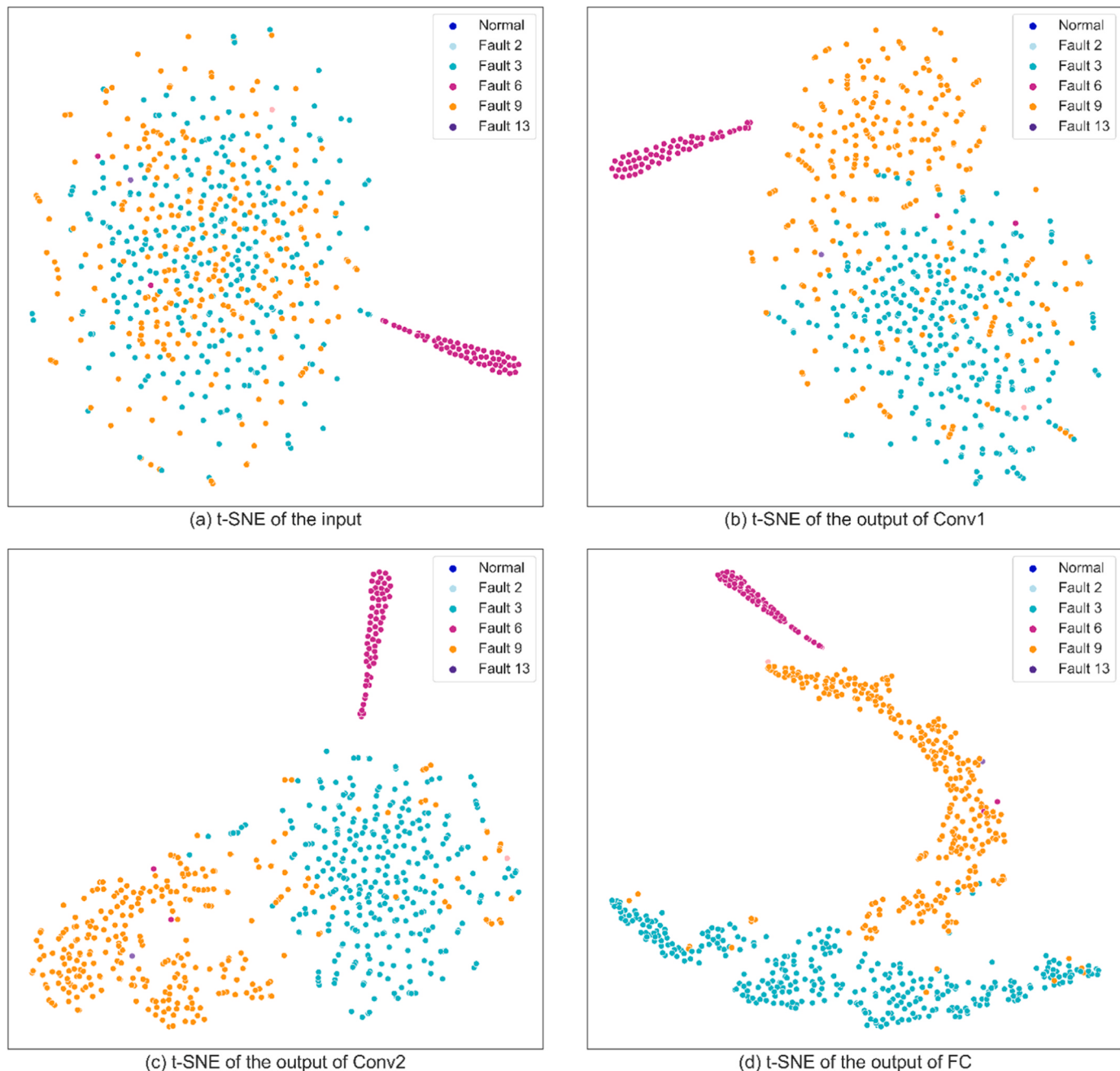


Fig. 13. Triage category 1 visualization using t-SNE.

5. Conclusions

This study proposes a Triage-based 1D-CNN model for fault diagnosis. The model utilizes a triage layer to determine the fault's triage type for timely warning, and sub networks layer to identify the specific fault type for accurate diagnosis. The 1D-CNN is employed to extract temporal features from the chemical process data. For complex chemical engineering processes, existing methods of fault diagnosis which model all faults with the same network and identical features are limited in diagnostic capability due to the limitations of model capacity. From a risk engineering perspective, triage-based fault diagnosis is better suited for complex chemical engineering processes.

Experimental results demonstrate the effectiveness and applicability of the TrCNN in the TE process. The triage layer achieves a fault detection rate (FDR) of 97%, enabling timely and accurate warnings. On

average, the overall FDR for the 15 known fault types reaches 96.78%. The model also exhibits good performance in early fault diagnosis. Additionally, the t-SNE visualization technique is utilized to visualize the hierarchical feature learning process of the model, and most of the data clusters are clear and accurate. The TrCNN offers advantages such as high fault diagnosis accuracy, reliability, and timely warnings, making it promising for industrial applications. Compared to other deep learning models such as LSTM and CNN algorithms, this method achieves superior diagnostic accuracy and false alarm rates while providing timely fault warnings. To ensure process safety, methods need to detect faults earlier and with greater accuracy. TrCNN can achieve earlier and more precise fault diagnosis, making it well-suited for complex chemical processes. This capability aids operators in promptly addressing exceptions to prevent accidents and effectively managing the risks associated with complex processes. With this method we can build a more efficient

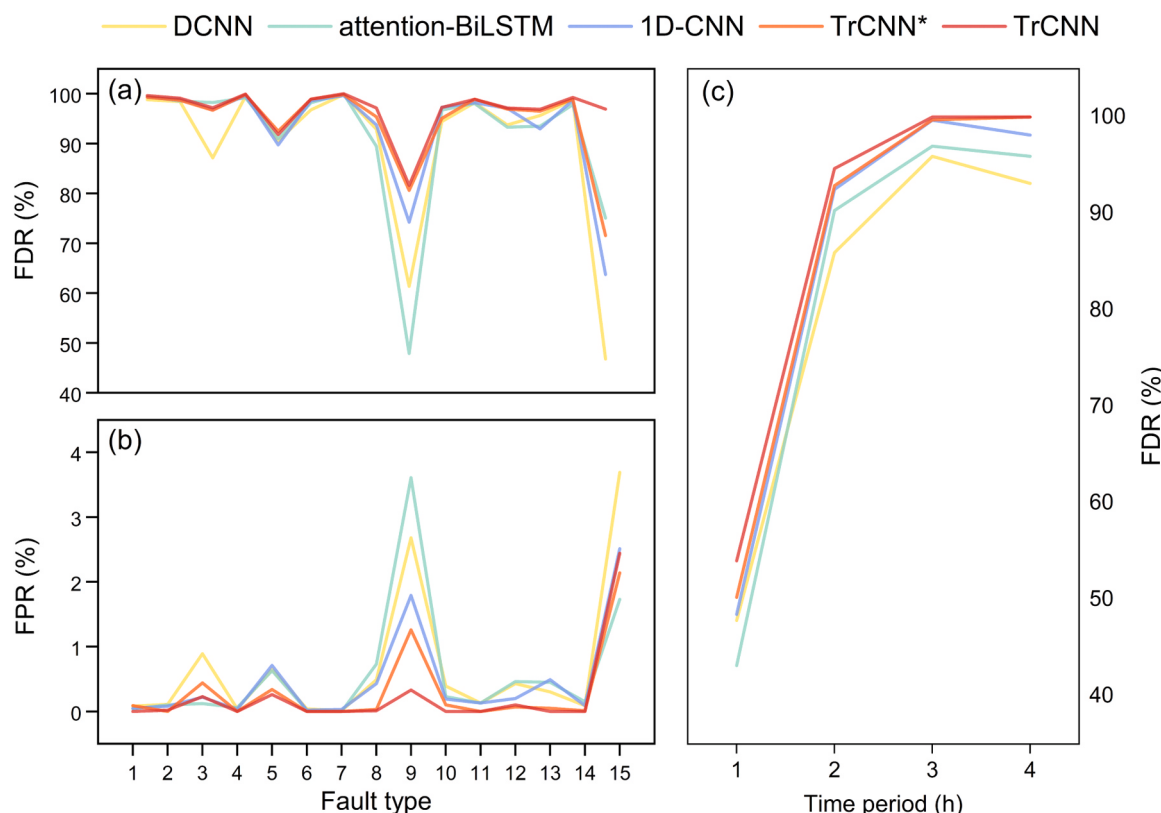


Fig. 14. The overall FDR (a.), FPR (b.), and FDR in different time period (c.) based on five methods.

Table 10

The average FDR of Unknown Fault Occurs.

Unknown Fault type	Fault 2	Fault 3	Fault 11	Fault 15
Average FDR (%)	76.19	99.13	77.44	85.63

and practical risk management system which has a substantial effect on process safety.

It should be noted that the fault diagnosis models presented in this study are data-driven. Future work can be carried out on exploring different models tailored to specific fault types based on application requirements. The method can be used as a general framework for fault diagnosis of various tasks in risk assessment.

Declaration of Competing Interest

The authors declare that they have no known competing financial interests or personal relationships that could have appeared to influence the work reported in this paper.

Acknowledgment

The authors are grateful for the support of the National Key Research and Development Program of China (2021YFB4000505).

Appendix A. Supporting information

Supplementary data associated with this article can be found in the online version at [doi:10.1016/j.psep.2024.01.072](https://doi.org/10.1016/j.psep.2024.01.072).

References

- Alauddin, M., Khan, F., Imtiaz, S., Ahmed, S., Amyotte, P., 2023. Integrating process dynamics in data-driven models of chemical processing systems. *Process Saf. Environ. Prot.* 174, 158–168.
- Amin, M.T., Khan, F., Ahmed, S., Imtiaz, S., 2021a. A data-driven Bayesian network learning method for process fault diagnosis. *Process Saf. Environ. Prot.* 150, 110–122.
- Amin, M.T., Khan, F., Ahmed, S., Imtiaz, S., 2021b. Risk-based fault detection and diagnosis for nonlinear and non-Gaussian process systems using R-vine copula. *Process Saf. Environ. Prot.* 150, 123–136.
- Arunthavarathan, R., Khan, F., Ahmed, S., Imtiaz, S., 2021. An analysis of process fault diagnosis methods from safety perspectives. *Comput. Chem. Eng.* 145, 107197.
- Bai, Y., Zhao, J., 2023. A novel transformer-based multi-variable multi-step prediction method for chemical process fault prognosis. *Process Saf. Environ. Prot.* 169, 937–947.
- Bathelt, A., Ricker, N.L., Jelali, M., 2015. Revision of the tennessee eastman process model. *IFAC-Pap.* 48, 309–314.
- Bi, X., Zhao, J., 2021. A novel orthogonal self-attentive variational autoencoder method for interpretable chemical process fault detection and identification. *Process Saf. Environ. Prot.* 156, 581–597.
- Bi, X., Qin, R., Wu, D., Zheng, S., Zhao, J., 2022. One step forward for smart chemical process fault detection and diagnosis. *Comput. Chem. Eng.* 164, 107884.
- Chen, C., Zhou, L., Ji, X., He, G., Dai, Y., Dang, Y., 2020. Adaptive Modeling Strategy Integrating Feature Selection and Random Forest for Fluid Catalytic Cracking Processes. *Ind. Eng. Chem. Res.* 59, 11265–11274.
- Chen, S., Yu, J., Wang, S., 2022. One-dimensional convolutional neural network-based active feature extraction for fault detection and diagnosis of industrial processes and its understanding via visualization. *ISA Trans.* 122, 424–443.
- Chiang, L.H., Kotanchek, M.E., Kordon, A.K., 2004. Fault diagnosis based on Fisher discriminant analysis and support vector machines. *Comput. Chem. Eng.* 28, 1389–1401.
- Cun, Y.L., Jackel, L.D., Boser, B., Denker, J.S., Graf, H.P., Guyon, I., Henderson, D., Howard, R.E., Hubbard, W., 1989. Handwritten digit recognition: applications of neural network chips and automatic learning. *IEEE Commun. Mag.* 27, 41–46.
- Deng, L., Zhang, Y., Dai, Y., Ji, X., Zhou, L., Dang, Y., 2021. Integrating feature optimization using a dynamic convolutional neural network for chemical process supervised fault classification. *Process Saf. Environ. Prot.* 155, 473–485.
- Downs, J.J., Vogel, E.F., 1993. A plant-wide industrial process control problem. *Comput. Chem. Eng.* 17, 245–255.
- Espuña, A., 2018. Preface: European symposium on computer-aided process engineering. *Ind. Eng. Chem. Res.* 57, 9737–9739.

- Feng, Z., Li, Y., Xiao, B., Sun, B., Yang, C., 2022. Process monitoring of abnormal working conditions in the zinc roasting process with an ALD-based LOF-PCA method. *Process Saf. Environ. Prot.* 161, 640–650.
- Gordon, C.A.K., Burnak, B., Onel, M., Pistikopoulos, E.N., 2020. Data-Driven Prescriptive Maintenance: Failure Prediction Using Ensemble Support Vector Classification for Optimal Process and Maintenance Scheduling. *Ind. Eng. Chem. Res.* 59, 19607–19622.
- Hu, J., Zhang, L., Cai, Z., Wang, Y., Wang, A., 2015. Fault propagation behavior study and root cause reasoning with dynamic Bayesian network based framework. *Process Saf. Environ. Prot.* 97, 25–36.
- Ji, C., Ma, F., Wang, J., Sun, W., Zhu, X., 2022. Statistical method based on dissimilarity of variable correlations for multimode chemical process monitoring with transitions. *Process Saf. Environ. Prot.* 162, 649–662.
- Jiang, Q., Yan, X., Li, J., 2016. PCA-ICA Integrated with Bayesian Method for Non-Gaussian Fault Diagnosis. *Ind. Eng. Chem. Res.* 55, 4979–4986.
- Jiao, J., Zhao, M., Lin, J., Liang, K., 2020. A comprehensive review on convolutional neural network in machine fault diagnosis. *Neurocomputing* 417, 36–63.
- Kaib, M.T.H., Kouadri, A., Harkat, M.F., Bensmail, A., Mansouri, M., 2023. Improving kernel PCA-based algorithm for fault detection in nonlinear industrial process through fractal dimension. *Process Saf. Environ. Prot.* 179, 525–536.
- Kari, T., He, Z., Rouzi, A., Zhang, Z., Ma, X., Du, L., 2023. Power transformer fault diagnosis using random forest and optimized kernel extreme learning machine. *Intell. Autom. Soft Comput.* 37, 691–705.
- Kopbayev, A., Khan, F., Yang, M., Halim, S.Z., 2022. Gas leakage detection using spatial and temporal neural network model. *Process Saf. Environ. Prot.* 160, 968–975.
- Kumar, S., Thennadil, S.N., Morris, A.J., Martin, E.B., 2003. Adaptive partial least squares with application to process monitoring. *IFAC Proc. Vol.* 36, 789–794.
- LeCun, Y., Bengio, Y., Hinton, G., 2015. Deep learning. *Nature* 521, 436–444.
- Lee, J., Cameron, I., Hassall, M., 2019. Improving process safety: what roles for Digitalization and Industry 4.0? *Process Saf. Environ. Prot.* 132, 325–339.
- Li, J., Huang, R., He, G., Liao, Y., Wang, Z., Li, W., 2021. A two-stage transfer adversarial network for intelligent fault diagnosis of rotating machinery with multiple new faults. *IEEE/ASME Trans. Mechatron.* 26, 1591–1601.
- Li, X., Liu, Y., Abbassi, R., Khan, F., Zhang, R., 2022. A Copula-Bayesian approach for risk assessment of decommissioning operation of aging subsea pipelines. *Process Saf. Environ. Prot.* 167, 412–422.
- Liu, N., Hu, M., Wang, J., Ren, Y., Tian, W., 2022a. Fault detection and diagnosis using Bayesian network model combining mechanism correlation analysis and process data: Application to unmonitored root cause variables type faults. *Process Saf. Environ. Prot.* 164, 15–29.
- Liu, N., Wang, J., Sun, S., Li, C., Tian, W., 2022b. Optimized principal component analysis and multi-state Bayesian network integrated method for chemical process monitoring and variable state prediction. *Chem. Eng. J.* 430, 132617.
- Liu, Y., Ge, Z., 2018. Weighted random forests for fault classification in industrial processes with hierarchical clustering model selection. *J. Process Control* 64, 62–70.
- Mahadevan, S., Shah, S.L., 2009. Fault detection and diagnosis in process data using one-class support vector machines. *J. Process Control* 19, 1627–1639.
- Quinones-Grueiro, M., Prieto-Moreno, A., Verde, C., Llanes-Santiago, O., 2019. Data-driven monitoring of multimode continuous processes: a review. *Chemom. Intell. Lab. Syst.* 189, 56–71.
- Sansana, J., Joswiak, M.N., Castillo, I., Wang, Z., Reis, M.S., 2021. Recent trends on hybrid modeling for Industry 4.0. *Comput. Chem. Eng.* 151, 107365.
- Song, Q., Jiang, P., 2022. A multi-scale convolutional neural network based fault diagnosis model for complex chemical processes. *Process Saf. Environ. Prot.* 159, 575–584.
- Wang, G., Liu, J., Li, Y., 2015. Fault diagnosis using kNN reconstruction on MRI variables. *J. Chemom.* 29, 399–410.
- Wang, N., Li, H., Wu, F., Zhang, R., Gao, F., 2021. Fault diagnosis of complex chemical processes using feature fusion of a convolutional network. *Ind. Eng. Chem. Res.* 60, 2232–2248.
- Wei, Z., Ji, X., Zhou, L., Dang, Y., Dai, Y., 2022. A novel deep learning model based on target transformer for fault diagnosis of chemical process. *Process Saf. Environ. Prot.* 167, 480–492.
- Wise, B.M., Ricker, N., Veltkamp, D., Kowalski, B.R., 1990. A theoretical basis for the use of principal component models for monitoring multivariate processes. *Process Control Qual.* 1, 41–51.
- Wu, D., Zhao, J., 2021. Process topology convolutional network model for chemical process fault diagnosis. *Process Saf. Environ. Prot.* 150, 93–109.
- Wu, D., Bi, X., Zhao, J., 2023. ProTopomer: toward understandable fault diagnosis combining process topology for chemical processes. *Ind. Eng. Chem. Res.* 62, 8350–8361.
- Wu, H., Zhao, J., 2018. Deep convolutional neural network model based chemical process fault diagnosis. *Comput. Chem. Eng.* 115, 185–197.
- Wu, Y., Zhao, R., Ma, H., He, Q., Du, S., Wu, J., 2022. Adversarial domain adaptation convolutional neural network for intelligent recognition of bearing faults. *Measurement* 195, 111150.
- Xiao, B., Li, Y., Sun, B., Yang, C., Huang, K., Zhu, H., 2021. Decentralized PCA modeling based on relevance and redundancy variable selection and its application to large-scale dynamic process monitoring. *Process Saf. Environ. Prot.* 151, 85–100.
- Yao, Y., Dai, Y., Zhao, J., 2022. An enhanced dynamic artificial immune system based on simulated vaccine for early fault diagnosis with limited data. *Process Saf. Environ. Prot.* 165, 908–919.
- Yin, Z., Hou, J., 2016. Recent advances on SVM based fault diagnosis and process monitoring in complicated industrial processes. *Neurocomputing* 174, 643–650.
- Yu, J., Zhang, C., Wang, S., 2020. Multichannel one-dimensional convolutional neural network-based feature learning for fault diagnosis of industrial processes. *Neural Comput. Appl.* 33, 3085–3104.
- Zhang, J., Zhang, M., Feng, Z., Ruifang, L.V., Lu, C., Dai, Y., Dong, L., 2023. Gated recurrent unit-enhanced deep convolutional neural network for real-time industrial process fault diagnosis. *Process Saf. Environ. Prot.* 175, 129–149.
- Zhang, S., Qiu, T., 2022a. A dynamic-inner convolutional autoencoder for process monitoring. *Comput. Chem. Eng.* 158, 107654.
- Zhang, S., Qiu, T., 2022b. Semi-supervised LSTM ladder autoencoder for chemical process fault diagnosis and localization. *Chem. Eng. Sci.* 251, 117467.
- Zhang, S., Bi, K., Qiu, T., 2020. Bidirectional recurrent neural network-based chemical process fault diagnosis. *Ind. Eng. Chem. Res.* 59, 824–834.
- Zhang, Z., Zhao, J., 2017. A deep belief network based fault diagnosis model for complex chemical processes. *Comput. Chem. Eng.* 107, 395–407.
- Zhao, L.-T., Yang, T., Yan, R., Zhao, H.-B., 2022. Anomaly detection of the blast furnace smelting process using an improved multivariate statistical process control model. *Process Saf. Environ. Prot.* 166, 617–627.
- Zheng, S., Zhao, J., 2022. A self-adaptive temporal-spatial self-training algorithm for semisupervised fault diagnosis of industrial processes. *IEEE Trans. Ind. Inform.* 18, 6700–6711.